Europe PMC Funders Group
Author Manuscript
Nature. Author manuscript; available in PMC 2014 October 03.

Published in final edited form as:
Nature. 2014 April 3; 508(7494): 55–60. doi:10.1038/nature13165.

Capillary pericytes regulate cerebral blood flow in health and disease

Catherine N. Hall[#1], **Clare Reynell**[#1], **Bodil Gesslein**[#2], **Nicola B. Hamilton**[#1], **Anusha Mishra**[#1], **Brad A. Sutherland**[3], **Fergus M. O'Farrell**[1], **Alastair M. Buchan**[3], **Martin Lauritzen**[2], and **David Attwell**[1]

[1]Department of Neuroscience, Physiology & Pharmacology University College London, Gower St., London, WC1E 6BT, UK

[2]Department of Neuroscience & Pharmacology and Center for Healthy Aging, and Department of Clinical Neurophysiology, Glostrup Hospital, University of Copenhagen, DK-2200 Copenhagen N, Denmark

[3]Acute Stroke Programme, Radcliffe Department of Medicine, University of Oxford, Oxford, OX3 9DU, UK

[#] These authors contributed equally to this work.

Abstract

Brain blood flow increases, evoked by neuronal activity, power neural computation and are the basis of BOLD functional imaging. It is controversial whether blood flow is controlled solely by arteriole smooth muscle, or also by capillary pericytes. We demonstrate that neuronal activity and the neurotransmitter glutamate evoke the release of messengers that dilate capillaries by actively relaxing pericytes. Dilation is mediated by prostaglandin E_2, but requires nitric oxide release to suppress vasoconstricting 20-HETE synthesis. *In vivo*, when sensory input increases blood flow, capillaries dilate before arterioles and are estimated to produce 84% of the blood flow increase. In pathology, ischaemia evokes capillary constriction by pericytes. We show that this is followed by pericyte death in rigor, which may irreversibly constrict capillaries and damage the blood-brain barrier. Thus, pericytes are major regulators of cerebral blood flow and initiators of functional imaging signals. Prevention of pericyte constriction and death may reduce the long-lasting blood flow decrease which damages neurons after stroke.

Pericytes are isolated contractile cells on capillaries which may regulate cerebral blood flow[1,2] (as well as stabilising newly-formed capillaries[3], maintaining the blood-brain barrier[4-6], contributing to the "glial scar" in pathology[7], and having stem cell properties[8]). Pericytes can be constricted and dilated by neurotransmitters *in vitro*[1,9], via poorly-understood signalling pathways, and capillary blood flow heterogeneity might reflect differences in pericyte tone[10-12]. Pericytes can constrict *in vivo*, but it was suggested[2] that they do not relax actively to increase blood flow[13]. Similar controversy surrounds the effect of pericytes on blood flow in pathology[14,15]. We have now characterised the responses of pericytes in the neocortex and cerebellum to neuronal activity and ischaemia. Surprisingly,

Correspondence and requests for materials should be addressed to; d.attwell@ucl.ac.uk or mlauritz@sund.ku.dk.
Author contributions All authors contributed to designing the study, doing the experiments, analysing the results and writing the paper.

Supplementary Information is linked to the online version of the paper at www.nature.com/nature.

Reprints and permissions information is available at www.nature.com/reprints

Competing financial interests: None

Europe PMC Funders Author Manuscripts
Europe PMC Funders Author Manuscripts

Europe PMC Funders Author Manuscripts

Europe PMC Funders Author Manuscripts

we demonstrate that pericytes are the first vascular elements to dilate during neuronal activity, making them the initiators of functional imaging signals. Furthermore, they die readily in ischaemia, which is expected to promote brain damage.

Signalling regulating pericyte dilation

We assessed the signalling systems dilating molecular layer capillaries in cerebellar slices[1], using 95% or 20% O_2 in the superfusate to produce a supra-normal or a physiological [O_2] in the slice[16,17]. Capillaries were defined as vessels <10μm in diameter lacking a continuous layer of smooth muscle. Their diameter was larger ($p=2.3\times10^{-4}$) at the lower [O_2] (5.36±0.30μm (n=59) in 20% and 4.07±0.14μm (n=154) in 95% O_2). Capillary pericytes can be identified by labelling for NG2 proteoglycan or the PDGFRβ receptor (Fig. 1a), or employing mice expressing DsRed under control of the NG2 promoter[18] (Fig. 1b, c), and are a different cell class from Iba1-expressing perivascular microglia/macrophages[19] (Fig. 1c). For neocortical capillaries in P21 rats the pericyte soma density was 2.2±0.2 per 100μm of capillary length (950μm of capillary analysed in each of 11 confocal stacks). Pericytes extend processes along and around vessels (Fig. 1a-c) which regulate capillary diameter.

Over 60 minutes without applying any drugs, capillary diameter was extremely stable (see Fig. 4 below). Applying noradrenaline (2μM), to mimic its release from the locus coeruleus *in vivo*, produced a sustained constriction mediated by pericytes[1] (Fig. 1d-e), which was not affected by [O_2] (Fig. 1f). Superimposing glutamate (500μM), to mimic neuronal glutamate release[13], dilated capillaries at pericyte locations[1] (Fig. 1d, g; Suppl. Video 1). As a percentage of the diameter without drugs, this dilation was twice as large with 20% as with 95% O_2 (Fig. 1h), possibly due to less production of vasoconstricting 20-HETE in low [O_2] (see below and Ext. Data Fig. 1). Independent of [O_2], most pericytes (72% in 95% O_2; 70% in 20% O_2) constricted >5% to noradrenaline, and dilated >5% to glutamate (63% in 95% O_2 (n=154); 66% in 20% O_2 (n=59)), and most pericytes that constricted to noradrenaline also dilated to glutamate (71% in 95% O_2; 78% in 20% O_2). Glutamate also dilated some capillaries in the absence of noradrenaline: in 20% O_2, 29% (7/24) of pericytes dilated >5%, which is less (Chi^2 p=0.005) than the 66% of pericytes that dilated >5% after applying noradrenaline. Below, noradrenaline was used to pre-constrict capillaries, to aid analysis of the signalling underlying glutamate-evoked dilation.

These experiments do not establish which cells the noradrenaline and glutamate act on, which may be neurons, astrocytes or pericytes themselves[13], to release the downstream messengers that control pericyte tone. We can, however, rule out the idea that noradrenaline generates 20-HETE to constrict pericytes, because blocking 20-HETE synthesis with 1μM HET0016 did not affect the noradrenaline-evoked constriction (Ext. Data Fig. 2b, g).

Glutamate releases nitric oxide (NO), a vasodilator, by activating NMDA receptors[13] and an NO donor (DETA-NONOate, 100μM) evoked capillary dilation (Ext. Data Fig. 2m). Blocking NO synthase with L-N^G-nitroarginine (L-NNA, 100μM) reduced the glutamate-evoked dilation (Fig. 1i, l; ANOVA p=0.002; L-NNA and other blockers used did not inhibit the noradrenaline-evoked constriction: Ext. Data Fig. 2). Surprisingly, the dilation was not affected by blocking guanylyl cyclase with ODQ (10μM, ANOVA p=1), so NO does not act by raising [cGMP] in the pericyte (Fig. 1j, m, Ext. Data Fig. 2e). However, when production of vasoconstricting 20-HETE was blocked using HET0016 (1μM), L-NNA no longer inhibited the dilation (Fig. 1k, n, ANOVA on black bars in l and n, p=0.0005), implying that NO promotes dilation by preventing 20-HETE formation. Since a robust dilation occurs with both NO and 20-HETE synthesis blocked (Fig. 1k, n), another messenger must be active. Blocking synthesis of epoxy-derivatives of arachidonic acid with MS-PPOH (10μM) did not affect the dilation (Ext. Data Fig. 2i, ANOVA p=0.92), but blocking EP_4 receptors for

Europe PMC Funders Author Manuscripts

Europe PMC Funders Author Manuscripts

prostaglandin E_2 (with 1μM L-161,982) greatly reduced it (Fig. 1o-p, ANOVA p=0.001). A similar inhibition of capillary dilation by blocking EP_4 receptors was seen in neocortical pericytes (Fig. 1q, p=0.004). Applying prostaglandin E_2 itself dilated cerebellar capillaries (Ext. Data Fig. 2n). We therefore identify the messenger that dilates capillaries in response to glutamate as prostaglandin E_2 (or a related species active at EP_4 receptors), but this dilation requires NO release to suppress 20-HETE formation (Ext. Data Fig. 1b).

Glutamate (500μM) or NMDA (100μM) (Fig. 2a-b, d), or parallel fibre stimulation (Fig. 2c-d), evoked an outward membrane current in pericytes patch-clamped at −55 to −75 mV (sometimes preceded by a small inward current: Ext. Data Fig. 3). The stimulation-evoked outward current was inhibited (paired t-test p=0.005) by blocking action potentials with TTX (Fig. 2c, reduced to 15±12% (n=4) of its amplitude without TTX, not significantly different from zero, p=0.28), whereas the NMDA-evoked current was unaffected by TTX (reduced by 12±19%, n=5, p=0.56), consistent with stimulation evoking the outward current by generating action potentials that release glutamate. The stimulation-evoked current of ~30pA is expected to hyperpolarize the cells by ~9mV (see Methods) and decrease voltage-gated Ca^{2+} entry, causing active relaxation[9] (although other Ca^{2+} sources, and cyclic nucleotides, may also regulate contractile tone[9,20]). Indeed, parallel fibre stimulation produced a dilation of 14.9±3.1% in 21 capillaries in 20% O_2 (Fig. 2e-h; Suppl. Video 2), which (unlike the noradrenaline-evoked constriction) was blocked by TTX and by blocking EP_4 receptors (Fig. 2g-h).

An outward current at negative potentials is not consistent with activation of glutamatergic ionotropic receptors, but is consistent with K^+ current activation. These data suggest that glutamate release generates PgE_2, which dilates the capillaries by activating an outward K^+ current in pericytes. PgE_2 similarly activates an outward K^+ current in aortic smooth muscle[21], and relaxes kidney pericytes[22].

Pericytes increase blood flow *in vivo*

To assess whether pericyte relaxation regulates blood flow *in vivo*, we electrically stimulated the whisker pad (at 3Hz) and used two-photon imaging of the vasculature (labelled with FITC-dextran) in somatosensory cortex to monitor dilations of penetrating arterioles (entering the cortex from the pia) and capillaries, in anaesthetised mice expressing DsRed in pericytes (Fig. 3a). The capillary diameter *in vivo* was 4.4±0.1 μm in 633 capillary regions (Ext. Data Table 1). Pericytes were visualised up to 200μm deep in the cortex (layer 2/3). Brief whisker pad stimulation (2s) evoked vessel dilations that peaked just after the end of the stimulation (~2.5s, Fig. 3b). Longer (15s) stimulation produced dilations that initially followed the same time course, then dilated further throughout the stimulation (Fig. 3b, Ext. Data Fig. 4). Most imaging employed 15s stimuli, which increased the response magnitude and measurement accuracy. Repeated stimulation gave reproducible responses (Ext. Data Fig. 5a-b). We segmented the vasculature by the branching order of the vessels, zero being the penetrating arteriole, one the primary capillary branching off the arteriole, etc. (see Ext. Data Fig. 1, and Ext. Data Table 1 for resting diameters, dilations and numbers of each vessel order). Whisker pad stimulation dilated vessels of all orders (Fig. 3c, Ext. Data Table 1). The fraction of vessels responding (i.e. with a dilation >5%) was similar in penetrating arterioles and in 1st order capillaries, while the frequency of capillary responses decreased with increasing order (Fig. 3c).

To establish where vasodilation is initiated, we imaged different orders of vessel simultaneously. Strikingly, 1st order capillaries usually dilated before penetrating arterioles (Fig. 3d-e; Suppl. Video 3), with vasodilation onset (assessed as the time to 10% of the maximum dilation) in the capillary being 1.38±0.38s earlier than for the penetrating arteriole

Europe PMC Funders Author Manuscripts

Europe PMC Funders Author Manuscripts

(Fig. 3e-f, p=0.015). Further along the vascular tree there was no significant difference in the time to dilation of simultaneously imaged capillaries of adjacent order (Fig. 3f, Ext. Data Fig. 5c). Thus, capillaries dilate before the penetrating arteriole feeding them. Averaging over all vessels of the same order (not just those imaged simultaneously) showed a similar faster dilation of capillaries than of penetrating arterioles (Fig. 3g), with the time to 10% of the maximum dilation for penetrating arterioles (3.7±0.3s) being significantly longer than the values (~2.7s) obtained for 1st and 2nd order capillaries (p=0.040 and 0.039 respectively, Fig. 3h, Ext. Data Fig. 5d). As expected, the time course of the blood flow increase in capillaries, assessed from the speed of red blood cell movement with line-scanning[23], increased with a time course similar to the capillary dilation (Ext. Data Fig. 5f).

The faster dilation in capillaries compared to arterioles indicates that capillary dilation is not a passive response to a pressure increase produced by arteriole dilation. To assess whether pericytes generate this dilation, we measured the diameter changes of capillaries at locations where DsRed-labelled pericytes were present (either somata or processes, responses did not differ significantly at these locations: Ext. Data Fig. 5e) or where no pericyte was visible. The resting diameter of capillaries was larger where pericyte somata or processes were present (4.62±0.09μm, n=464) than in pericyte-free zones (3.72±0.08μm, n=168, Mann-Whitney $p=2.7\times10^{-7}$), suggesting that pericytes induce an increase of capillary diameter. Dilations over 5% were much more frequent at pericyte locations (Fig. 3i; Chi^2 $p=7.5\times10^{-11}$), where the responses were also larger ($p=3.2\times10^{-5}$, Kolmogorov-Smirnov test: Fig. 3j-k). These data confirm that pericytes actively relax to generate the capillary dilation.

In ischaemia pericytes constrict and die

Does pericyte control of capillary diameter also play a role in pathology? Pericytes constrict some retinal capillaries in ischaemia[1], perhaps because pericyte $[Ca^{2+}]_i$ rises when ion pumping is inhibited by ATP depletion. Cortical capillaries also constrict following middle cerebral artery occlusion[14] (MCAO) *in vivo*. Clinically, reperfusion of thrombus-occluded arteries using tPA can be achieved in 1-6 hours[24,25] but, even when arterial flow is restored, a long-lasting reduction of cerebral blood flow can ensue[26-29]. This may reflect pericyte constriction outlasting ischaemia[14], but it is unclear why the constriction is so prolonged. We examined the effect of ischaemia on pericyte health using propidium iodide to mark cell death.

Live imaging of cerebral cortical slices exposed to simulated ischaemia (oxygen-glucose deprivation with ATP synthesis by glycolysis and oxidative phosphorylation inhibited with iodoacetate and antimycin) revealed that, within ~15 mins, grey matter capillaries constricted at spatially-restricted regions near pericytes (Fig. 4a-c). In contrast, the diameter of capillaries not exposed to ischaemia was stable over 60 mins (reduced by 3.2±3.0%, p=0.31, n=13, Fig. 4c). While capillaries not exposed to ischaemia showed little pericyte death even after one hour (as assessed by propidium iodide labelling), ischaemia led to most pericytes on capillaries dying after ~40 mins, usually at locations where the earlier constriction had occurred. All capillaries exposed to ischaemia that we examined showed a consistent response, in which the pericytes first constricted the capillaries, and then died (Fig. 4c). Death of pericytes in rigor, after they have been constricted by a loss of energy supply, should produce a long-lasting increase in the resistance of the capillary bed.

To sample more pericytes than is possible while live imaging the capillary diameter, and examine mechanisms contributing to their death, we acquired confocal stacks of brain slices exposed to simulated ischaemia, which were then fixed and labelled for NG2 and/or isolectin B_4. Ischaemia led to pericytes apposed to capillaries dying rapidly in both the white

Europe PMC Funders Author Manuscripts

Europe PMC Funders Author Manuscripts

matter of the cerebellum (Fig. 5a-b) and the grey matter of the cerebral cortex (Fig. 5c-d). For pericytes exposed to simulated ischaemia as above, ~90% of pericytes died within an hour (Fig. 5b). This was unaffected by blocking action potentials (with TTX, 1μM) but was halved by blocking AMPA/kainate (25μM NBQX) or NMDA receptors (50μM D-AP5, 50μM MK-801 and 100μM 7-chlorokynurenate), implying an excitotoxic contribution to pericyte death. When oxygen-glucose deprivation (OGD) alone was employed (without antimycin and iodoacetate), to allow ATP generation when oxygen and glucose were restored, ~40% of pericytes died after one hour, but OGD-evoked death increased 1.5-fold during 1 hour of reperfusion (Fig. 5c-d). Ionotropic glutamate receptor block or removal of external Ca^{2+} again significantly reduced the death (Fig. 5d), while blocking NO production had a small protective effect and lowering free radical levels by scavenging $O_2^{\cdot -}$. had no significant effect (Fig. 5d, Ext. Data Fig. 6a). Blocking metabotropic glutamate receptors or 20-HETE production, which might prevent $[Ca^{2+}]_i$ rises, or blocking mitochondrial calcium uptake, also had no effect (Ext. Data Fig. 6b).

Pericytes apposed to capillaries, unlike endothelial cells, also died *in vivo* after 90 min of middle cerebral artery occlusion (MCAO, followed by 22.5 hours recovery: Fig. 5e-f, Ext. Data Fig. 6c). In contrast, a sham operation occluding only the internal carotid artery (see Methods) produced less pericyte death, and a sham operation with no artery occlusion (which did not affect blood flow: see Methods) induced no more death than in naive untreated animals. Thus, pericyte death is a rapid response of the cerebral vascular bed to ischaemia, both in brain slices and *in vivo*.

Discussion

Understanding what initiates the blood flow increase in response to neuronal activity is crucial for understanding both how information processing is powered and how functional imaging signals are generated[30]. Most neurons are closer to capillaries (~8.4μm distant, in hippocampus[31]) than to arterioles (70μm distant[31]), suggesting that neurons might adjust their energy supply by initially signalling to pericytes (Ext. Data Fig. 1a). Our data support this concept: neuronal activity leads to a release of messengers that activate an outward membrane current in pericytes (Fig. 2) and dilates capillaries before arterioles (Fig. 3). Capillary dilation implies that there is a resting tone set by the pericytes, perhaps as a result of noradrenaline release from locus coeruleus axons, two thirds of the perivascular terminals of which end near capillaries rather than arterioles[32]. Vascular diameter responses can propagate between adjacent pericytes[1,9], but it is not yet known whether arterioles receive a signal to dilate from pericytes, or from vasoactive messengers which reach arterioles later than they reach pericytes. We have identified the cause of pericyte dilation as being EP_4 receptor activation, by PgE_2 or a related compound, although NO production is also needed to suppress synthesis of vasocontricting 20-HETE (Fig. 1, Ext. Data Fig. 1b). These mechanisms resemble those controlling arteriole dilation, and may reflect glutamate release activating the production of arachidonic acid and its derivatives in astrocytes or neurons[13].

The more frequent occurrence of capillary dilation at pericyte locations (Fig. 3i-k), and the faster onset of capillary dilation than of arteriole dilation *in vivo* (Fig. 3d-h) suggest that pericytes actively relax to dilate capillaries. Our data suggest that capillaries have two conceptually separate roles in regulating cerebral blood flow. First, being closer to neurons, they detect neuronal activity earlier than arterioles can, and may pass a hyperpolarizing vasodilatory signal back to arterioles (via gap junctions between pericytes or endothelial cells)[1,9]. Second, capillary vasodilation itself contributes significantly to increasing blood flow. To assess the extent to which capillary dilations increase blood flow, we used data on the vascular tree in mouse cortex[33] (see Methods). For a mean arteriole dilation of 5.9% during prolonged (15s) stimulation (Ext. Data Table 1), a capillary dilation of 6.7%

Europe PMC Funders Author Manuscripts

Europe PMC Funders Author Manuscripts

(averaged over all capillary orders, Ext. Data Table 1) and ignoring venule dilation, the steady state blood flow was predicted to increase by 19%. Omitting the capillary dilation predicted a flow increase of only 3%. Thus, capillary dilation is estimated to generate 100× (19-3)/19=84% of the steady state increase in blood flow evoked by neuronal activity, and capillaries dilate ~1s before penetrating arterioles (Fig. 3d-h). These results suggest that BOLD functional imaging signals largely reflect capillary dilation by pericytes.

For ischaemia, our data support, but modify, the suggestion that pericyte constriction[1,14] may be a cause of the long-lasting decrease of cerebral blood flow that occurs even when a blocked artery is opened up after stroke[26-29]. Whereas it was previously envisaged that constriction of capillaries was by healthy pericytes and could be reversed by suppressing oxidative stress[14], we find that, after ischaemia has constricted them (Fig. 4), pericytes die readily (Fig. 5). This death is mediated in part by glutamate, but is not reduced by free radical scavenging, suggesting that the constriction and death differ at least partly in their causes. Pericyte death in rigor will produce a long-lasting decrease of capillary blood flow[26-29], as well as a breakdown of the (pericyte-maintained[4-6]) blood-brain barrier. Both of these will contribute to ongoing neuronal damage, highlighting the potential importance of preventing pericyte death as a therapeutic strategy after stroke, particularly in the penumbra of an affected region. To develop this approach, it will be necessary to develop small molecule inhibitors of pericyte death that could be administered, perhaps with tissue plasminogen activator, soon after a stroke has occurred.

Methods

Animals

Experiments used Sprague-Dawley or Wistar rats and NG2-DsRed C57BL/6J mice of either sex. Animal procedures were carried out in accordance with the guidelines of the UK Animals (Scientific Procedures) Act 1986, the Danish National Ethics Committee and European Directive 2010/63/EU. Each experiment was conducted on tissue from at least 3 animals on at least 3 different experimental days.

Brain slice preparation

Slices (200-300 μm thick) were prepared[35] on a vibratome in ice cold oxygenated (95% O_2/5% CO_2) solution. This solution was usually artificial CSF (aCSF) containing (in mM) 124 NaCl, 2.5 KCl, 26 $NaHCO_3$, 1 $MgCl_2$, 1 NaH_2PO_4, 10 glucose, 0.1-1 Na ascorbate, 2 $CaCl_2$ (to which 1 kynurenic acid was added to block glutamate receptors), and slices were incubated at room temperature in the same solution until used in experiments. For Fig. 2e-h, the slicing solution contained (mM) 93 N-methyl-D-glucamine chloride, 2.5 KCl, 30 $NaHCO_3$, 10 $MgCl_2$, 1.2 NaH_2PO_4, 25 glucose, 0.5 $CaCl_2$, 20 HEPES, 5 Na ascorbate, 3 Na pyruvate, 1 kynurenic acid, and the slices were incubated at 34°C in the same solution for 10 mins, and then incubated at room temperature until used in experiments in a similar solution with the NMDG-Cl, $MgCl_2$, $CaCl_2$ and Na ascorbate replaced by (mM) 92 NaCl, 1 $MgCl_2$ 2 $CaCl_2$ and 1 Na ascorbate.

Immunohistochemical labelling of pericytes

Isolectin B_4 binds to α-D-galactose residues in the basement membrane secreted by endothelial cells[36,37], which surrounds pericytes. Cerebellar slices were incubated in FITC-conjugated 10 μg/ml isolectin B_4 (Sigma) for one hour then fixed for 20 mins in 4% PFA, and incubated for 4-6 hrs in 0.05% Triton X-100, 10% goat serum in phosphate-buffered saline at 21°C, then with primary antibody at 21°C overnight with agitation, and then for 4-8 hrs at 21°C with secondary antibody. Primary antibodies were: guinea pig NG2 (from W.B. Stallcup, 1:100), rabbit NG2 (Millipore AB5320, 1:300) and rabbit PDGFRβ (Santa Cruz

Europe PMC Funders Author Manuscripts

Europe PMC Funders Author Manuscripts

sc432, 1:200). Secondary antibodies (goat) were: anti-rabbit (Molecular Probes, 1:200) and anti-guinea pig (Jackson Lab, 1:100). Pericytes, with a bump on a log morphology on capillaries, or located at the junction of capillaries, labelled for NG2 and PDGFRβ (Fig. 1). Since perivascular immune cells are sometimes confused with pericytes[19], we labelled the former with antibody to Iba1 (rabbit Iba1, Synaptic Systems 234003, 1:500) in 7 cortical and 8 cerebellar slices from 5 NG2-DsRed animals, and found that none of 135 (cortex) and 212 (cerebellum) NG2-DsRed labelled perivascular cells co-labelled for Iba1 (although Iba1 labelled 110 cells in the cortical slices and 136 cells in the cerebellar slices, Fig. 1c), implying that pericytes defined by an on-capillary location and NG2 expression differ from perivascular microglia/macrophages.

Imaging capillaries in brain slices

Slices were perfused with bicarbonate-buffered aCSF, as described above, but without the kynurenic acid, at 31-35°C. In experiments using 20% oxygen, the perfusion solution was bicarbonate-buffered aCSF, gassed with 20% O_2, 5% CO_2, and 75% N_2.

For bright-field recording of capillary diameter, sagittal cerebellar slices were prepared from postnatal day 10 (P10)-P21 Sprague-Dawley rats or coronal cortical slices were prepared from P12 rats. On average 1.3 capillary regions were imaged per slice. Capillaries were imaged[1] at ~30 μm depth within the molecular layer of cerebellar slices or the grey matter of somatosensory/motor cortex slices, using a x40 water immersion objective, a Coolsnap HQ2 CCD camera, and ImagePro Plus or Metafluor acquisition software. Images were acquired every 1-5 sec, with an exposure time of 5 msec. Pixel size was 160 or 300 nm. Vessel internal diameters were measured by manually placing a measurement line (perpendicular to the vessel, Fig. 1d) on the image (at locations near visible pericytes which constricted when noradrenaline was applied), using ImagePro Analyzer, Metamorph or ImageJ software, with the measurer blinded as to the timing of drug applications. The end of the measurement line was placed at locations representing the measurer's best estimate of where the rate of change of intensity was greatest across pixels under the vessel edge, and diameter was estimated to a precision of one pixel. Where necessary, images were aligned by manually tracking drift, or by using Image Pro "Align Global Images" macro. Experiments where changes in focus occurred were excluded from further analysis. Data in the presence of blockers of signalling pathways were compared with interleaved data obtained without the blockers.

For experiments in which the parallel fibres were stimulated in the molecular layer, coronal slices were used to preserve the parallel fibres, and stimuli of 60-100 μs duration, at 50–90 V and 12 Hz, were applied for 25 sec using a patch pipette electrode placed approximately 100 μm away from the imaged vessel. To check that parallel fibres were being successfully activated, the field potential was monitored in the molecular layer using a 4 MΩ patch pipette filled with aCSF. To ensure that pericytes were healthy we excluded capillaries that did not constrict to 1 μM noradrenaline. Stimulation evoked a dilation (Fig. 2e, f) except in 2 capillaries which constricted, presumably due to direct depolarization of a pericyte by the stimulus since when TTX was applied (to one of these vessels) a stimulation-evoked constriction was still seen in TTX: these 2 vessels were excluded from the analysis.

Patch-clamp recordings of pericytes

Coronal slices of cerebellum were prepared[35] from P10-P17 NG2-DsRed C57BL/6J mice. Slices were superfused with bicarbonate-buffered solution containing (mM) 124 NaCl, 26 $NaHCO_3$, 1 NaH_2PO_4, 2.5 KCl, 1 $MgCl_2$, 2.5 $CaCl_2$, 10 glucose, bubbled with 95% O_2/5% CO_2, pH 7.3, at 21-23°C or 33-36°C (stimulation evoked currents were not significantly different at the two temperatures and were pooled). Pericytes were identified as DsRed-expressing cells located on capillaries (oligodendrocyte precursor cells also express NG2-

Europe PMC Funders Author Manuscripts

Europe PMC Funders Author Manuscripts

DsRed but these can be distinguished from pericytes morphologically and by their position in the parenchyma). Pericytes were whole-cell clamped between −55 and −75 mV with pipettes containing solution comprising (mM) 130 K-gluconate, 4 NaCl, 0.5 $CaCl_2$, 10 HEPES, 10 BAPTA, 2 Na_2ATP, 2 $MgCl_2$, 0.5 Na_2GTP, 0.05 Alexa Fluor 488, pH set to 7.3 with KOH. Electrode junction potentials were compensated. Patch-clamped cells were morphologically confirmed to be pericytes by dye filling. Series resistance was 20-40 MΩ. In 17 cells the mean resting potential was −47.6±2.1 mV, and the mean input resistance at the resting potential was 292±27 MΩ. A 30 pA outward current evoked by neuronal activity (see main text) is thus expected to hyperpolarise pericytes by ~9mV.

Imaging of vessels *in vivo*

Animal preparation—16 adult NG2 DsRed C57BL/6J mice (18-37 g, of either sex) were prepared for experiments by cannulation of the trachea for mechanical ventilation (SAR-830; CWE, Ardmore, PA). Catheters were placed into the left femoral artery and vein and perfused with physiological saline. The end-expiratory CO_2 (microCapstar End-tidal CO_2 Monitor, CWE) and blood pressure (Pressure Monitor BP-1; World Precision Instruments, Sarasota, FL) were monitored continuously in combination with blood gases in arterial blood samples (pO_2 115-130 mm Hg; pCO_2 35-40 mm Hg; pH 7.35-7.45; ABL 700 Series; Radiometer Medical, Brønshøj, Denmark) to ensure the animals were kept under physiological conditions. The temperature was measured and maintained at 37°C during the experiment with a rectal thermometer regulated heating pad (TC-1000 Temperature Controller; CWE). The animals were anaesthetized with xylazine (10 mg/kg i.p.) and ketamine (60 mg/kg i.p.) during surgery, and then switched to alpha-chloralose (50 mg/kg/h i.v.) during the experiment. The skull was glued to a metal plate using cyanoacrylate gel (Loctite Adhesives) and the plate was fixed in the experimental setup. A craniotomy was drilled with a diameter of approximately 4 mm with the center 0.5 mm behind and 3 mm to the right of the bregma over the sensory barrel cortex region. The dura was removed and the preparation covered with 0.75% agarose (type III-A, low EEO; Sigma-Aldrich, St. Louis, MO) and moistened with artificial cerebrospinal fluid (in mM: 120 NaCl, 2.8 KCl, 22 $NaHCO_3$, 1.45 $CaCl_2$, 1 Na_2HPO_4, 0.9 $MgCl_2$ and 2.6 glucose; pH=7.4) at 37°C and bubbled with 95% air/5% CO_2. The craniotomy was covered with a glass coverslip. When experiments were complete, mice were euthanized by intravenous injection of anaesthesia (pentobarbital, 200 mg/ml and lidocaine hydrochloride, 20 mg/ml) followed by decapitation.

Whisker pad stimulation—The mouse sensory barrel cortex was activated by stimulation of the contralateral ramus infraorbitalis of the trigeminal nerve using a set of custom-made bipolar electrodes inserted percutaneously. The cathode was positioned at the hiatus infraorbitalis (IO), and the anode was inserted into the masticatory muscles[38]. Thalamocortical IO stimulation was performed at an intensity of 1.5 mA (ISO-flex; AMPI, Jerusalem) and lasting 1 ms, in trains of 2 sec or 15 sec at 3 Hz. The stimulation was controlled by a sequencer file running within Spike2 software (version 7.02; Cambridge Electronic Design, England).

Cortical response imaging—For each animal, the haemodynamic response to stimulation was detected using intrinsic optical imaging (IOS) and used to identify the region of brain activated by whisker pad stimulation, for further vascular imaging. Two photon imaging of blood vessels was then conducted near the centre of this activated region. The IOS was recorded on a Leica microscope with 4× magnification that included the entire preparation in the field of view. The light source consisted of LEDs with green light filters and a fast camera (QuantEM 512SC; Photometrics, Tucson) sampled 29 images/sec before and during 15 sec of 3 Hz stimulation. As haemoglobin strongly absorbs green light, the captured light intensity decreases as the total haemoglobin concentration increases during

Europe PMC Funders Author Manuscripts

Europe PMC Funders Author Manuscripts

changes in cerebral blood volume and flow[39]. Images during stimulation were subtracted from control images[40], allowing the area of brain where blood flow increases during whisker stimulation to be revealed.

2-photon imaging—2% w/v fluorescein isothiocyanate-dextran (FITC-dextran, MW 70,000, 50 μl, Sigma-Aldrich) was administered into the femoral vein to label the blood plasma. *In vivo* imaging of blood vessel diameter and pericyte location was performed using a commercial two-photon microscope (SP5, Leica, Wetzlar, Germany), a MaiTai HP Ti:Sapphire laser (Millennia Pro; Spectra Physics, Santa Clara, CA, mean output power 10mW), and a 20× 1.0 N.A. water-immersion objective (Leica). Tissue was excited at 900 nm wavelength, and the emitted light was filtered to collect red and green light from DsRed (pericytes) and FITC-dextran (vessel lumens). Penetrating arterioles were identified unequivocally *in vivo* in two ways, firstly by tracing their connections back to pial arterioles with obvious smooth muscle around them, and secondly by observing the direction of flow of the red blood cells from the arterioles into the parenchymal capillaries. Z-stack images were taken of the area of interest. XY-time series were taken to image pericytes and blood vessels during stimulation, with a frame size 512 × 300 pixels (170 msec/frame; pixel size was 93-201 nm depending on the magnification used, with a mean value of 155 nm; pixel dwell time was 1.1 μsec).

Image analysis—The presence of red blood cells (RBCs) leads to apparent holes in the images of the capillary and (to a lesser extent) the arteriole (Ext. Data Fig. 4a-b). This image noise was reduced by smoothing images with a maximum intensity 10 frame (1.7 sec) running summation of the green channel showing the FITC-labelled vascular lumen (see Ext. Data Fig. 4a-d for sample images, and the effect this would have on the apparent timing of a step increase of diameter and on the dilations shown in Fig. 3d). This channel was then processed to extract blood vessel diameters. Lines were placed across the vessel (perpendicular to the vessel wall) at a spacing of ~20 μm (e.g. Fig. 3d). The edges of the vessel were located using the ImagePro caliper tool, which finds the greatest gradient in light intensity along the line (where $d^2\text{intensity}/dx^2=0$). As for brain slice imaging above, interpolation of the image intensity across pixels allows, in principle, the position of the edge to be estimated to change by less than one pixel, but in practice we measured the diameter with a precision of one pixel. We considered whether the smoothing applied could artefactually preferentially accelerate the dilation seen for capillaries. In fact this is not possible, because the smoothing uses a maximum intensity sum of all the 10 frames: consequently, a black area produced by a passing RBC will not add to the summed image, and any increase in diameter that has occurred will only be detected in a later frame. Thus, passage of a RBC can only delay the apparent time at which dilation is detected, this effect should be larger in capillaries in which the RBCs are moving more slowly, and yet the capillaries dilate before the arterioles (Fig. 3). We conclude that the smoothing cannot cause a preferential acceleration of the time course of dilation in the capillary data. For Fig. 3e and g the time courses of the measured diameter were also smoothed with a 5 point FFT procedure that removes frequencies over 1.16 Hz (OriginLab software), the effect of which is shown in Ext. Data Fig. 4e. Responding capillaries were defined as those showing a change upon stimulation of more than 5% of the initial vessel diameter (since 4.99% was twice the standard deviation of the baseline diameter averaged over all vessels studied). Where multiple regions responded on a single vessel, their response times were averaged for comparison between paired vessels (Fig. 3f and Ext. Data Fig. 5c). Blood flow in capillaries was assessed from the velocity of RBCs, which appear as dark patches inside FITC-dextran labelled vessels, using line-scan imaging[23]. Repetitive line-scans (0.358 ms/line of 512 pixels) along the axis of the vessel before, during and after whisker stimulation (3Hz, 15s) were used to form a space-time image in which moving RBCs produce streaks with a slope

that is equal to the inverse of the speed. The slope was calculated using an automated image-processing algorithm[41]. The baseline speed of RBCs averaged over all capillaries studied was 1.73±0.20 mm/sec (n=49).

Cell death experiments

Chemical ischaemia—For chemical ischaemia experiments (Figs. 4, 5a-b), sagittal cerebellar slices from P21 (Fig. 4) or P7 (Fig. 5a-b) Sprague-Dawley rats were incubated at 37°C in an ischaemic solution in which glucose was replaced with 7 mM sucrose and oxygen was removed by equilibrating solutions with 5% CO_2 and 95% N_2. In addition, 2 mM iodoacetate and 25 μM antimycin were added to the ischaemic solution to block ATP generation by glycolysis and oxidative phosphorylation, respectively[42]. Control slices were incubated in aCSF, gassed as usual with 5% CO_2, 95% O_2. Propidium iodide (PI, 37 μM) was added to both solutions to label dead cells. After 60 min incubation in this ischaemic solution, slices were fixed for 20 minutes in 4% paraformaldehyde and immunohistochemistry for NG2 was performed, as described above.

Oxygen-glucose deprivation—For the oxygen-glucose deprivation experiments shown in Fig. 5c-d, coronal forebrain slices were prepared from P21 Sprague Dawley rats then incubated in aCSF in which glucose was replaced with 7 mM sucrose and oxygen was removed by equilibrating solutions with 5% CO_2 and 95% N_2. Control slices were incubated in aCSF, gassed as usual with 5% CO_2, 95% O_2. After 60 min, some slices were immediately fixed in 4% paraformaldehyde, while others were placed in control aCSF, to reoxygenate for a further 60 min. All solutions also contained 37 μM PI and 10 μg/ml FITC-conjugated isolectin B_4 to label dead cells and blood vessels, respectively. Slices were swiftly washed in aCSF prior to fixation for 20 min in 4% paraformaldehyde, washed 3 times in PBS and mounted on microscope slides in Dako hard set mounting medium. Slides were then imaged using a Zeiss LSM 700 or 710 confocal microscope. PI-positive dead vascular and parenchymal cells were counted using ImageJ software, by an experimenter who was blind to their condition. Cells in the 20 μm closest to the slice surface were excluded from analysis to prevent confounds from slicing-induced damage. Dead or alive pericytes were identified by their “bump on a log” morphology on vessels surrounded by isolectin B_4 labelling. To check that pericytes could be identified by isolectin B_4 labelling alone, in parallel experiments we labelled slices for isolectin B_4 and NG2: the great majority (93% of 718 cells assessed) of pericytes identified this way were found to be positive for NG2. Although some pericytes may slightly move away from capillaries after hypoxia or brain injury[43,44], we only counted pericytes apposed to capillaries in this study.

Middle cerebral artery occlusion—Male Wistar rats (Harlan, UK) weighing 253-312g, housed on a 12h light/dark cycle with *ad libitum* access to food and water, underwent transient middle cerebral artery occlusion (MCAO) as previously described[45]. In brief, animals were anaesthetised with 4% isoflurane and maintained in 1.5-2% isoflurane carried in 70% N_2O and 30% O_2. A midline incision was made in the neck, the right external carotid artery was cauterised and cut, and the right common carotid and internal carotid arteries were temporarily ligated. Through a small arteriotomy in the external carotid artery stump, a 4-0 nylon filament coated with silicone at the tip (Doccol, USA) was advanced up the internal carotid artery to occlude the right middle cerebral artery at its origin. For sham animals, the entire procedure was followed except that either: (i) the filament was only advanced up the beginning of the internal carotid artery (ICA) before being withdrawn after 3 mins (sham with ICA occlusion), or (ii) the external carotid artery was permanently ligated (which had no effect on cerebral blood flow) and the common and internal carotid arteries were exposed but not ligated, and the animals remained under anaesthesia for the same length of time as sham animals (sham without ICA occlusion). Core temperature was

Europe PMC Funders Author Manuscripts
Europe PMC Funders Author Manuscripts

Europe PMC Funders Author Manuscripts

Europe PMC Funders Author Manuscripts

maintained at 37°C by a rectal thermister probe attached to a heating pad. Cerebral blood flow was continuously monitored by placing a laser Doppler probe (Oxford Optronix, Oxford, UK) over a thinned skull of the MCA territory approximately 4 mm lateral and 1.5 mm caudal to bregma. In MCAO animals, averaged over the period of occlusion, cerebral blood flow on the treated side fell to 34.9±7.1 % of baseline (n=6) for 90 mins, while in sham animals with ICA occlusion it dropped significantly less to 67.9±11.0% of baseline (n=3, t-test p=0.035) for 16 mins (this smaller drop occurs because of occlusion of the ICA), and in sham animals without ICA occlusion blood flow was unaffected (104.0±3.9% of baseline, n=3). Following 90 minutes of MCAO, the filament was retracted, and the common carotid artery ligation was released to allow maximal reperfusion. Anaesthesia was then removed, and at 22.5 hours of reperfusion, neurological deficit was assessed by investigating limb symmetry, motor function, activity and sensory stimulation (modified from ref. 46). A maximum score of 15 equates to severe neurological deficit, while a minimum score of 0 implies no neurological deficit. MCAO animals had a mean score of 7.5±1.7 (n=6), which was significantly greater than that of sham animals with ICA occlusion (0.3±0.3, n=3, p=0.027) and sham animals without ICA occlusion (0±0, n=3 p=0.039, corrected for multiple comparisons). Animals (including an additional 3 naïve control animals) were then anaesthetised, decapitated, and 200 μm forebrain slices were prepared on a vibratome and labelled with PI and FITC-isolectin B_4 in aCSF for 60 min, then washed, fixed, mounted and cortical and striatal images were captured as described above. Live and dead pericytes were counted in both regions as above except that dead endothelial cells were also counted (identified by their elongated nuclei). More pericyte death was seen in brain slices made from naïve control animals in this *in vivo* series of experiments (Fig. 5f) than in experiments studying pericyte death in slices (Fig. 5b, d); this may be because, for the adult rats used for the *in vivo* experiments, it takes longer to kill the animal and remove its brain, than for the younger animals used for slice experiments. The total number of endothelial cells present, and therefore the percentage of dead endothelial cells, was estimated from the total number of pericytes, assuming a 1:3 ratio of pericytes to endothelial cells[47].

Statistics

Data are mean±s.e.m. P values are from ANOVA (univariate, unless otherwise stated) and post-hoc Dunnett's or Student's t-tests, Chi^2 tests, Kolmogorov–Smirnov tests or Mann-Whitney U tests (for non-normally distributed data), as appropriate. Two-tailed tests were used. P values quoted in the text are from independent samples t-tests unless otherwise stated. For multiple comparisons, p values are corrected using a procedure equivalent to the Holm-Bonferroni method (for N comparisons, the most significant p value is multiplied by N, the 2nd most significant by N-1, the 3rd most significant by N-2, etc.; corrected p values are significant if they are less than 0.05). Normality of data was assessed using Kolmogorov–Smirnov tests. All statistical analysis was conducted using IBM SPSS21 or OriginLab software.

Contribution of capillary dilation to cerebral blood flow increases

To assess how capillary dilations increase blood flow in the steady state, we used data from a recent analysis of the vascular tree in mouse cortex[33]. For blood flow from the cortical surface (where for simplicity we assume blood pressure to be constant) through a penetrating arteriole to layer 4 of the cortex, through the array of inter-connected capillaries, and back to the cortical surface through a penetrating venule, that analysis[33] concluded that the resistances (at baseline diameter) of the arteriole, capillary and venule segments of this path were, respectively, 0.1, 0.4 (for a path from an arteriole to a venule separated by ~200 μm, Figs. 5c and 2g of Ref. 34) and 0.2 poise/μm^3, so that capillaries provide 57% of the total resistance. For a mean neuronal activity evoked arteriole dilation of 5.9% during prolonged (15 sec) stimulation (Table 1 of main text), a capillary dilation of 6.7% (averaged

Europe PMC Funders Author Manuscripts

Europe PMC Funders Author Manuscripts

over all capillary orders, Table 1) and ignoring venule dilation, then for resistance inversely proportional to the 4th power of diameter (Poiseuille's law) the blood flow should increase by 19% in the steady state. Omitting the capillary dilation predicts a flow increase of only 3%, while omitting the arteriole dilation (so that only capillaries dilate) predicts a flow increase of 15%. Deviations from Poiseuille's law in the capillaries[33] make only a small correction to these values. Thus, capillary dilation is predicted to generate 84% of the steady state increase in blood flow evoked by prolonged neuronal activity. This figure would be reduced somewhat if pial arteriole dilation[48] significantly contributes to the flow increase. For example if pial arterioles are assumed to dilate by the same 5.9% as penetrating arterioles, and to have the same resistance as penetrating arterioles, then the capillary contribution to the blood flow increase is predicted to be 73% (however the larger diameter of pial vessels and their anastomoses[49] suggest that their contribution to the total resistance and blood flow control will be much less than that of the penetrating arterioles).

Relationship to earlier work

A previous failure to observe active capillary dilation[2] may reflect two factors. Firstly, in that study[2], unlike ours, the authors were unable to reproducibly evoke blood flow increases by whisker pad stimulation and so used bicuculline to excite neurons: conceivably this induces seizure-like activity which may generate a non-physiological release of vasoconstricting 20-HETE, as well as of dilating messengers. Secondly, the use of thiopental anaesthetic in that study[2] may have reduced blood flow increases, since the same group reported that the closely related anaesthetic thiobutabarbital suppresses neuronally-evoked blood flow increases by 40% compared to those seen using α-chloralose (the anaesthetic that we use)[50]. In addition, the vessels they define as precapillary arterioles[2] (their Fig. 4h), which did show active dilations, appear to have isolated pericytes on them (rather than continuous smooth muscle) and would be called 1st order capillaries in our nomenclature.

Duration of rigor after pericyte death

Rigor occurs because when the ATP level falls muscle cells like pericytes cannot detach their myosin heads from actin to relax. At the whole body level rigor mortis following death (the stiffness resulting from skeletal muscles dying in rigor) lasts about 18-36 hours, depending on temperature. We would therefore expect pericytes to stay in rigor for hours (i.e. the period after ischaemia for which blood flow is known to be reduced[26]), unless removed by microglia.

Supplementary Material

Refer to Web version on PubMed Central for supplementary material.

Acknowledgments

We thank Beverley Clark, Alasdair Gibb, Alex Gourine, Clare Howarth, Renaud Jolivet, Christian Madry, Peter Mobbs, Bill Richardson and Angus Silver for comments on the manuscript. Supported by the Fondation Leducq, European Research Council, Wellcome Trust, UK Medical Research Council, Nordea Foundation via Center for Healthy Aging, the Lundbeck Foundation, NOVO-Nordisk Foundation and Danish Medical Research Council.

References

1. Peppiatt CM, Howarth C, Mobbs P, Attwell D. Bidirectional control of CNS capillary diameter by pericytes. Nature. 2006; 443:700–704. [PubMed: 17036005]
2. Fernández-Klett F, Offenhauser N, Dirnagl U, Priller J, Lindauer U. Pericytes in capillaries are contractile *in vivo*, but arterioles mediate functional hyperemia in the mouse brain. Proc. Natl. Acad. Sci. U.S.A. 2010; 107:22290–22295. [PubMed: 21135230]

Europe PMC Funders Author Manuscripts

Europe PMC Funders Author Manuscripts

3. Chan-Ling T, Page MP, Gardiner T, Baxter L, Rosinova E, Hughes S. Desmin ensheathment ratio as an indicator of vessel stability: evidence in normal development and in retinopathy of prematurity. Am. J. Pathol. 2004; 165:1301–1313. [PubMed: 15466395]
4. Bell RD, Winkler EA, Sagare AP, Singh I, LaRue B, Deane R, Zlokovic BV. Pericytes control key neurovascular functions and neuronal phenotype in the adult brain and during brain aging. Neuron. 2010; 68:409–427. [PubMed: 21040844]
5. Armulik A, Genové G, Mäe M, Nisancioglu MH, Wallgard E, Niaudet C, He L, Norlin J, Lindblom P, Strittmatter K, Johansson BR, Betsholtz C. Pericytes regulate the blood-brain barrier. Nature. 2010; 468:557–561. [PubMed: 20944627]
6. Daneman R, Zhou L, Kebede AA, Barres BA. Pericytes are required for blood-brain barrier integrity during embryogenesis. Nature. 2010; 468:562–566. [PubMed: 20944625]
7. Göritz C, Dias DO, Tomilin N, Barbacid M, Shupliakov O, Frisén J. A pericyte origin of spinal cord scar tissue. Science. 2011; 333:238–242. [PubMed: 21737741]
8. Dore-Duffy P, Katychev A, Wang X, Van Buren E. CNS microvascular pericytes exhibit multipotential stem cell activity. J. Cereb. Blood Flow Metab. 2006; 26:613–624. [PubMed: 16421511]
9. Puro DG. Physiology and pathobiology of the pericyte-containing retinal microvasculature: new developments. Microcirculation. 2007; 14:1–10. [PubMed: 17365657]
10. Villringer A, Them A, Lindauer U, Einhäupl K, Dirnagl U. Capillary perfusion of the rat brain cortex. An in vivo confocal microscopy study. Circ Res. 1994; 75:55–62. [PubMed: 8013082]
11. Schulte ML, Wood JD, Hudetz AG. Cortical electrical stimulation alters erythrocyte perfusion pattern in the cerebral capillary network of the rat. Brain Res. 2003; 963:81–92. [PubMed: 12560113]
12. Jespersen SN, Østergaard L. The roles of cerebral blood flow, capillary transit time heterogeneity, and oxygen tension in brain oxygenation and metabolism. J. Cereb. Blood Flow Metab. 2012; 32:264–277. [PubMed: 22044867]
13. Attwell D, Buchan A, Charpak S, Lauritzen M, MacVicar BA, Newman EA. Glial and neuronal control of blood flow. Nature. 2010; 468:232–243. [PubMed: 21068832]
14. Yemisci M, Gursoy-Ozdemir Y, Vural A, Can A, Topalkara K, Dalkara T. Pericyte contraction induced by oxidative-nitrative stress impairs capillary reflow despite successful opening of an occluded cerebral artery. Nat. Med. 2009; 15:1031–1037. [PubMed: 19718040]
15. Vates GE, Takano T, Zlokovic B, Nedergaard M. Pericyte constriction after stroke: the jury is still out. Nat. Med. 2010; 16:959. [PubMed: 20823870]
16. Hall CN, Klein-Flügge MC, Howarth C, Attwell D. Oxidative phosphorylation, not glycolysis, powers presynaptic and postsynaptic mechanisms underlying brain information processing. J. Neurosci. 2012; 32:8940–8951. [PubMed: 22745494]
17. Hall CN, Attwell D. Assessing the physiological concentration and targets of nitric oxide in brain tissue. J. Physiol. 2008; 586:3597–3615. [PubMed: 18535091]
18. Zhu X, Bergles DE, Nishiyama A. NG2 cells generate both oligodendrocytes and gray matter astrocytes. Development. 2008; 135:145–157. [PubMed: 18045844]
19. Krueger M, Bechmann I. CNS pericytes: concepts, misconceptions, and a way out. Glia. 2010; 58:1–10. [PubMed: 19533601]
20. Hamilton NB, Attwell D, Hall CN. Pericyte-mediated regulation of capillary diameter: a component of neurovascular coupling in health and disease. Front. Neuroenergetics. 2010; 2:5. doi: 10.3389/fnene.2010.00005. [PubMed: 20725515]
21. Serebryakov V, Zakharenko S, Snetkov V, Takeda K. Effects of prostaglandins E_1 and E_2 on cultured smooth muscle cells and strips of rat aorta. Prostaglandins. 1994; 47:353–365. [PubMed: 8066184]
22. Crawford C, Kennedy-Lydon T, Sprott C, Desai T, Sawbridge L, Munday J, Unwin RJ, Wildman SSP, Peppiatt-Wildman CM. An intact kidney slice model to investigate vasa recta properties and function in situ. Nephron Physiol. 2012; 120:17–31.
23. Kleinfeld D, Mitra PP, Helmchen F, Denk W. Fluctuations and stimulus-induced changes in blood flow observed in individual capillaries in layers 2 through 4 of rat neocortex. Proc. Natl. Acad. Sci. U.S.A. 1998; 95:15741–15746. [PubMed: 9861040]

Europe PMC Funders Author Manuscripts

Europe PMC Funders Author Manuscripts

24. Khatri P, et al. Good clinical outcome after ischemic stroke with successful revascularization is time-dependent. Neurology. 2009; 73:1066–1072. [PubMed: 19786699]
25. Gupta, et al. Higher volume endovascular stroke centers have faster times to treatment, higher reperfusion rates and higher rates of good clinical outcomes. J. Neurointervent. Surg. 2013; 5:294–297.
26. Hauck EF, Apostel S, Hoffmann JF, Heimann A, Kempski O. Capillary flow and diameter changes during reperfusion after global cerebral ischemia studied by intravital video microscopy. J. Cereb. Blood Flow Metab. 2004; 24:383–391. [PubMed: 15087707]
27. Leffler CW, Beasley DG, Busija DW. Cerebral ischemia alters cerebral microvascular reactivity in newborn pigs. Am. J. Physiol. 1989; 257:H266–271. [PubMed: 2750942]
28. Nelson CW, Wei EP, Povlishock JT, Kontos HA, Moskowitz MA. Oxygen radicals in cerebral ischemia. Am. J. Physiol. 1992; 263:H1356–1362. [PubMed: 1332509]
29. Baird AE, Donnan GA, Austin MC, Fitt GJ, Davis SM, McKay WJ. Reperfusion after thrombolytic therapy in ischemic stroke measured by single-photon emission computed tomography. Stroke. 1994; 25:79–85. [PubMed: 8266387]
30. Attwell D, Iadecola C. The neural basis of functional imaging signals. Trends Neurosci. 2002; 25:621–625. [PubMed: 12446129]
31. Lovick TA, Brown LA, Kay BJ. Neurovascular relationships in hippocampal slices: physiological and anatomical studies of mechanisms underlying flow-metabolism coupling in intraparenchymal microvessels. Neuroscience. 1999; 92:47–60. [PubMed: 10392829]
32. Cohen Z, Molinatti G, Hamel E. Astroglial and vascular interactions of noradrenaline terminals in the rat cerebral cortex. J. Cereb. Blood Flow Metab. 1997; 17:894–904. [PubMed: 9290587]
33. Blinder P, Tsai PS, Kaufhold JP, Knutsen PM, Suhl H, Kleinfeld D. The cortical angiome: a 3-D interconnected vascular network with noncolumnar patterns of blood flow. Nature Neurosci. 2013; 16:889–897. [PubMed: 23749145]
34. Mathiesen C, Brazhe A, Thomsen K, Lauritzen M. Spontaneous calcium waves in Bergmann glia increase with age and hypoxia and may reduce tissue oxygen. J. Cereb. Blood Flow Metab. 2013; 33:161–169. [PubMed: 23211964]

Methods and Extended Data References

35. Marcaggi P, Attwell D. Endocannabinoid signaling depends on the spatial pattern of synapse activation. Nature Neurosci. 2005; 8:776–781. [PubMed: 15864304]
36. Peters BP, Goldstein IJ. The use of fluorescein-conjugated Bandeiraea simplicifolia B4-isolectin as a histochemical reagent for the detection of alpha-D-galactopyranosyl groups. Their occurrence in basement membranes. Exp. Cell Res. 1979; 120:321–334. [PubMed: 436961]
37. Laitinen L. Griffonia simplicifolia lectins bind specifically to endothelial cells and some epithelial cells in mouse tissues. Histochem. J. 1987; 19:225–234. [PubMed: 3597137]
38. Norup Nielsen A, Lauritzen M. Coupling and uncoupling of activity-dependent increases of neuronal activity and blood flow in rat somatosensory cortex. J. Physiol. 2001; 533:773–785. [PubMed: 11410634]
39. Frostig RD, Lieke EE, Ts'o DY, Grinvald A. Cortical functional architecture and local coupling between neuronal activity and the microcirculation revealed by in vivo high-resolution optical imaging of intrinsic signals. Proc. Natl. Acad.Sci. U.S.A. 1990; 87:6082–6086. [PubMed: 2117272]
40. Harrison TC, Sigler A, Murphy TH. Simple and cost-effective hardware and software for functional brain mapping using intrinsic optical signal imaging. J. Neurosci. Methods. 2009; 182:211–218. [PubMed: 19559049]
41. Schaffer CB, Friedman B, Nishimura N, Schroeder LF, Tsai PS, Ebner FF, Lyden PD, Kleinfeld D. Two-photon imaging of cortical surface microvessels reveals a robust redistribution in blood flow after vascular occlusion. PLoS Biol. 2006; 4:e22. [PubMed: 16379497]
42. Allen NJ, Káradóttir R, Attwell D. A preferential role for glycolysis in preventing the anoxic depolarization of rat hippocampal area CA1 pyramidal cells. J. Neurosci. 2005; 25:848–859. [PubMed: 15673665]

Europe PMC Funders Author Manuscripts

Europe PMC Funders Author Manuscripts

43. Dore-Duffy P, Owen C, Balabonov R, Murphy S, Beaumont T, Rafols JA. Pericyte migration from the vascular wall in response to traumatic brain injury. Microvasc. Res. 2000; 60:55–69. [PubMed: 10873515]
44. Gonul E, Duz B, Kahraman S, Kayali H, Kubar A, Timurkaynak E. Early pericyte response to brain hypoxia in cats: an ultrastructural study. Microvasc. Res. 2002; 64:116–119. [PubMed: 12074637]
45. Nagel S, Papadakis M, Chen R, Hoyte LC, Brooks KJ, Gallichan D, Sibson NR, Pugh C, Buchan AM. Neuroprotection by dimethyloxalylglycine following permanent and transient focal cerebral ischemia in rats. J. Cereb. Blood Flow Metab. 2011; 31:132–143. [PubMed: 20407463]
46. Garcia JH, Wagner S, Liu KF, Hu XJ. Neurological deficit and extent of neuronal necrosis attributable to middle cerebral artery occlusion in rats. Statistical validation. Stroke. 1995; 26:627–634. [PubMed: 7709410]
47. Pardridge WM. Blood-brain barrier biology and methodology. J. Neurovirol. 1999; 5:556–569. [PubMed: 10602397]
48. Iadecola C, Yang G, Ebner TJ, Chen G. Local and propagated responses evoked by focal synaptic activity in cerebellar cortex. J. Neurophysiol. 1997; 78:651–659. [PubMed: 9307102]
49. Blinder P, Shih AY, Rafie C, Kleinfeld D. Topological basis for the robust distribution of blood to rodent neocortex. Proc. Natl. Acad. Sci., U.S.A. 2010; 107:12670–12675. [PubMed: 20616030]
50. Lindauer U, Villringer A, Dirnagl U. Characterization of CBF response to somatosensory stimulation: model and influence of anesthetics. Am. J. Physiol. 1993; 264:H1223–1228. [PubMed: 8476099]

Europe PMC Funders Author Manuscripts

Europe PMC Funders Author Manuscripts

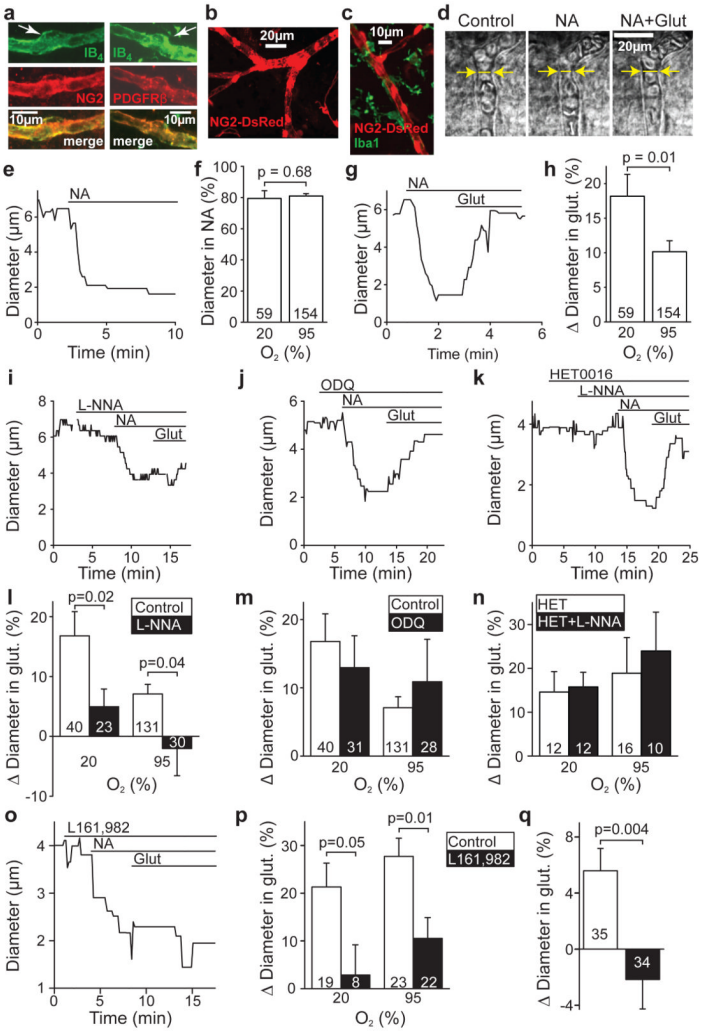

Figure 1. Signalling pathways controlling capillary diameter

a Capillaries in the molecular layer of rat cerebellum labelled using isolectin B_4; pericytes (arrow) labelled with NG2 or PDGFRβ antibodies. **b** Cerebellar capillaries in NG2-DsRed mouse; pericytes are red. **c** Neocortical capillaries in NG2-DsRed mouse; microglia labelled for Iba1. **d** Rat cerebellar capillary response to 2μM noradrenaline (NA) and superimposed 500μM glutamate (Glut). Line shows lumen diameter. **e** NA-evoked prolonged constriction (95% O_2; a large constriction is shown for clarity). **f** Diameter in NA was not affected by [O_2] (graphs show percentage of baseline diameter before drugs). **g** Glut dilates capillaries (20% O_2; a large dilation is shown for clarity). **h** Dilation was larger in low [O_2]. **i** NOS blocker L-N^G-nitroarginine (L-NNA, 100μM) inhibits Glut-evoked dilation (20% O_2). **j** Guanylyl cyclase blocker ODQ (10μM) does not block dilation (20% O_2). **k** Blocking 20-HETE production (HET0016, 1μM) abolishes the inhibitory effect of L-NNA (20% O_2). **l** L-NNA reduces Glut-evoked dilations at high and low [O_2] (ANOVA p=0.002; p values from post-hoc t-tests). **m** ODQ does not affect Glut-evoked dilation. **n** HET0016 abolishes effect of L-NNA. **o, p** Blocking EP_4 receptors (L161,982, 1μM) inhibits Glut-evoked dilation (o, 20% O_2) at high and low [O_2] (p). Data in d-p are from rat cerebellar capillaries. **q** EP_4 block abolishes Glut-evoked dilation in rat neocortical capillaries (20% O_2). Drug effects on baseline diameter are in Ext. Data Fig. 2.

Europe PMC Funders Author Manuscripts

Europe PMC Funders Author Manuscripts

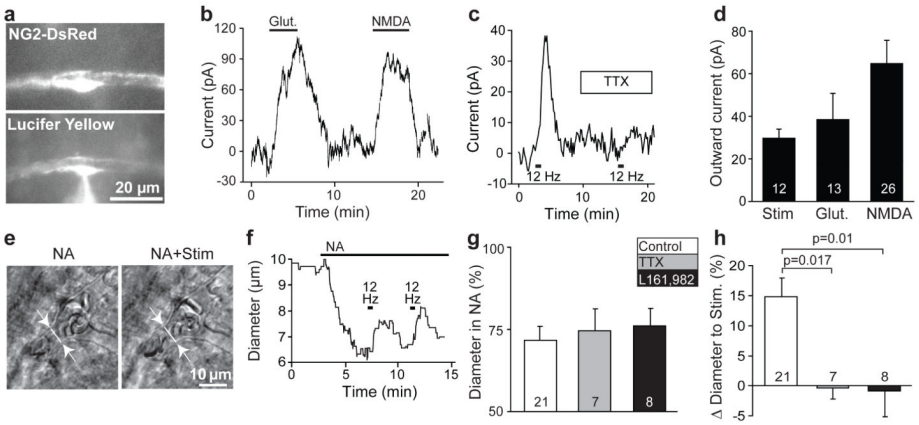

Figure 2. Pericyte membrane current and capillary dilation in cerebellar slices

a DsRed-labelled patch-clamped pericyte in molecular layer of mouse cerebellum. Lucifer yellow from pipette overlaps with DsRed. **b** Glutamate (Glut, 500μM) and NMDA (100μM) evoked outward current (−55mV). **c** Parallel fibre stimulation-evoked outward current (−74mV) is blocked by 1μM TTX. **d** Mean outward currents evoked by stimulation, glutamate and NMDA (b-d are in 95% O_2). **e-f** Parallel fibre stimulation (in NA 1 μM) in rat cerebellar slice evokes capillary dilation (20% O_2). **g-h** Constriction by NA (g) was unaffected by TTX or EP_4 block (L161,982), which abolished the stimulation-evoked dilation (h). P values from one-way ANOVA with Dunnett's post-hoc tests.

Europe PMC Funders Author Manuscripts

Europe PMC Funders Author Manuscripts

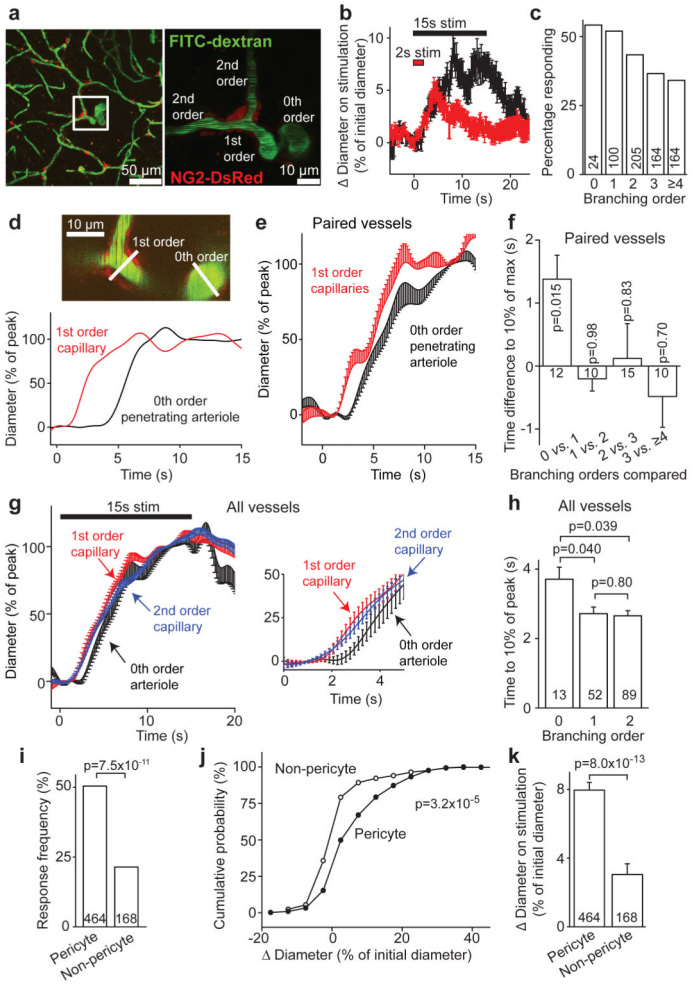

Figure 3. Active dilation of capillaries by pericytes *in vivo* in mouse cerebral cortex

a Confocal stack (90μm thick, maximum intensity projection) of FITC-dextran-filled vessels *in vivo* in somatosensory cortex of NG2-DsRed mouse (pericytes are red). Enlargement (single image) shows a penetrating arteriole (0th order) giving off a capillary (1st order) which splits into 2nd order branches. **b** Response of 45 capillary regions to 2s and 15s whisker pad stimulation. **c** Percentage of vessel regions of different orders (number studied on bars) showing >5% dilation to stimulation. **d** Simultaneous imaging (top, lines show measurement loci) of penetrating arteriole and 1st order capillary: capillary dilates 3s before arteriole (bottom: smoothing in d-g is explained in Methods and Ext. Data Fig. 4). **e** Dilation time course in simultaneously-imaged penetrating arterioles and 1st order capillaries. **f** Time to 10% of peak dilation for (j-1)th order (3rd order for j≥4) vessel minus that of jth order vessel. Capillaries dilate faster than arterioles. **g** Dilation time course in all responding (>5%) penetrating arterioles and 1st and 2nd order capillaries. Inset expands initial response. **h** Time to 10% of peak dilation in all 0th-2nd order responding vessels. **i** Percentage of capillary locations with or without pericytes showing >5% dilations. **j** Cumulative probability of capillary diameter changes (including "non-responding" capillaries with <5% dilations) in 464 pericyte and 168 non-pericyte locations. Diameter changes <0% (constrictions) represent random changes and measurement error. **k** Mean responses for distributions in j (p from Mann-Whitney U-test).

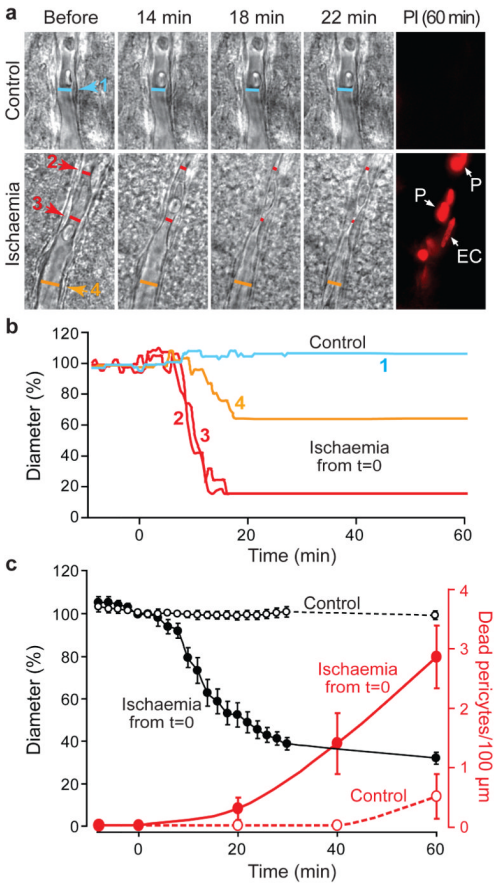

Figure 4. In ischaemia, pericytes constrict capillaries and then die in rigor

a Top: capillary in a rat cortical slice in normal solution. Bottom: capillary exposed to simulated ischaemia. Right: propidium iodide (PI) labelling after one hour, showing dead pericytes (P) and endothelial cell (EC). **b** Vessel diameters in a, at regions indicated, over time. **c** Mean diameter and number of dead pericytes/(100 μm) from 9 capillaries in ischaemia (measured at 18 locations) and 6 capillaries in normal solution (13 locations). Diameter in ischaemia was reduced from control ($p=1.3\times10^{-15}$ and $7.7.\times10^{-17}$ at 30 and 60 mins). Pericyte death was higher in ischaemia at 40 and 60 mins (Mann-Whitney p=0.041 and 0.021). A few pericytes also died on capillaries in non-ischaemic slices, but did not constrict capillaries (1.3±1.5 % diameter decrease at 3 dead pericytes on 2 vessels).

Europe PMC Funders Author Manuscripts

Europe PMC Funders Author Manuscripts

Europe PMC Funders Author Manuscripts

Europe PMC Funders Author Manuscripts

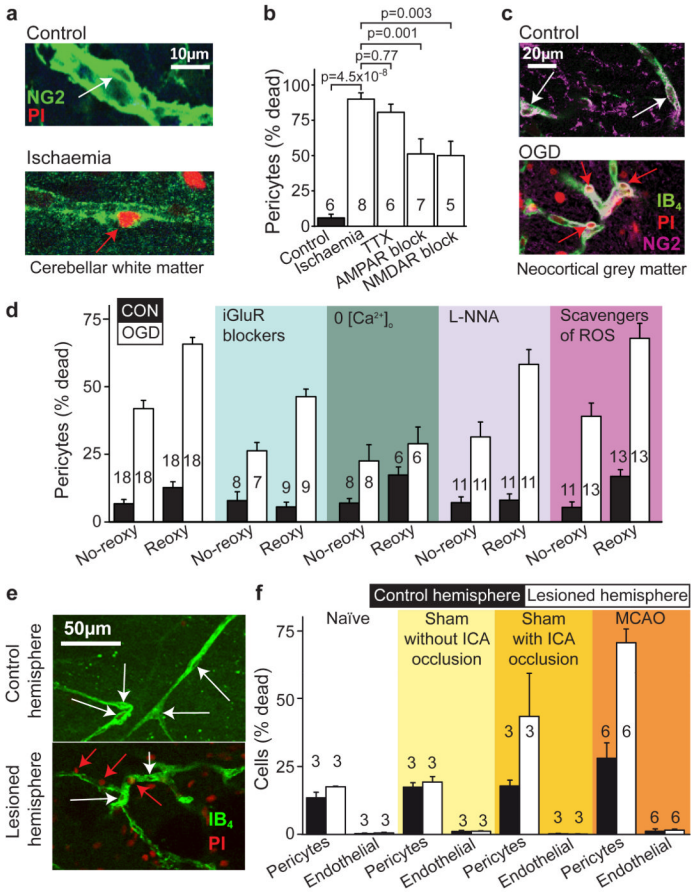

Figure 5. Pericyte death in ischaemia

a Rat cerebellar slice white matter capillaries labelled for NG2 and propidium iodide (PI) after 1 hour of control (white arrow: living pericyte) or ischaemia solution containing antimycin and iodoacetate (red arrow: dead pericyte). **b** Percentage of pericytes dead in control or after 1 hour's ischaemia (as in a) alone or with block of action potentials (TTX, 1μM), AMPA/kainate receptors (25μM NBQX), or NMDA receptors (50μM D-AP5, 50μM MK-801, 100μM 7-chlorokynurenate); p values from one-way ANOVA with Dunnett's post-hoc tests. **c** Rat neocortical slice grey matter capillaries labelled for IB_4, NG2 and PI after 1 hour's control solution or oxygen+glucose deprivation (OGD). **d** Percentage of pericytes (as in c) dead after one hour's OGD (No-reoxy) or OGD followed by 1 hour of control solution (Reoxy) with no drugs, or with iGluR block (NBQX (25μM), AP5 (50μM) and 7CK (100μM)), zero $[Ca^{2+}]_o$, NOS block (100μM L-NNA), or free radical scavenging (150μM MnTBAP or 100μM PBN, pooled data from Ext. Data Fig. 5a) throughout. OGD killed pericytes (ANOVA, $p=10^{-13}$) and death increased during reperfusion ($p=3.3\times10^{-13}$). iGluR block or zero $[Ca^{2+}]_o$ reduced death (ANOVA with Dunnett's post-hoc test, $p=2.7\times10^{-4}$ and 6.0×10^{-7}). Blocking NOS had a small protective effect (p=0.026); ROS scavenging did not (p=0.99). **e-f** Confocal images of striatal capillaries labelled with IB_4 and PI (e) and percentage of striatal pericytes and endothelial cells that are dead (f) from the control and lesioned hemisphere of *in vivo* MCAO-treated rats (90 mins, assessed 22.5 hours later), sham-operated rats (with or without filament being inserted into the internal carotid artery (ICA)), and naïve control animals. More pericytes die than endothelial cells (repeated measures ANOVA, $p=10^{-6}$). For pericytes, but not endothelial cells, cell death is greater in lesioned hemisphere (main effect of hemisphere, p=0.004; hemisphere-cell type interaction

p=0.003) and cell death is greater in MCAO-lesioned animals than in naïve or sham animals without ICA occlusion (Tukey post-hoc tests, p=0.005 and 0.01). See Ext. Data Fig. 5 for data from cortex.

Europe PMC Funders Author Manuscripts

Europe PMC Funders Author Manuscripts